SPACE TELESCOPE SCIENCE INSTITUTE
Operated for NASA by AURA

Instrument Science Report WFC 2013-14

Astrometric Correction for WFC3/UVIS Lithographic-Mask Pattern

V. Kozhurina-Platais, D. Hammer, N. Dencheva, & W. Hack

July 9, 2013

Abstract

Observations of the central field in ω Cen taken with large dither patterns and over a large range of HST roll-angles exposed through F606W UVIS filter have been used to examine the lithographic-mask pattern imprinted on the WFC3/UVIS detector during the manufacturing process. This detector defect introduces fine-scale astrometric errors at the level of about 0.2 pixel with a complicated spatial structure across the WFC3/UVIS CCD chips. The fine-scale solution was utilized to construct a 2–D look-up table for correction of the WFC3/UVIS lithographic-mask pattern. The astrometric errors due to this detector defect have been corrected down to the ∼0.05 pixel level. The derived 2–D look-up table can be interpolated at any point in the WFC3/UVIS image by ST software DrizzlePac/AstroDrizzle. The main results of these calibrations are: 1) new polynomial coefficients of geometric distortion for 14 calibrated UVIS filters in the form of Instrument Distortion Correction Table (IDCTAB file) were improved to account for the lithographic-mask pattern in the WFC3/UVIS detector; 2) new derived look-up table in the form of a D2IMFILE, which significantly improves (30-60%) the fine-scale structure in the WFC3/UVIS geometric distortion; 3) geometric distortion coupled with the D2IMFILE and new improved IDCTAB can now be successfully corrected to the precision level of ∼ 0.05 pixel (2 mas) for the UVIS detector.

1. Introduction

It is well–known that HST imaging instruments, such as WFPC2, ACS/WFC, and WFC3/UVIS & IR, have strong geometric distortion due to the optical assembly of the

telescope. By design, the focal plane of the WFC3/UVIS and IR cameras is tilted with respect to the incoming beam at ∼21° and ∼24°, respectively. As a result, the WFC3/UVIS and IR images are distorted by up to of ∼ 7% across the detector, which corresponds to 120 pixels or ∼5″ in the UVIS and 35 pixels or ∼4″ in the IR channel.

The knowledge of geometric distortion of the WFC3/UVIS and IR is the backbone of the STSDAS software Multidrizzle (Fruchter & Hook, 2002, Koekemoer, 2002, and Fruchter & Sosey *et al.*, 2009) and the recently improved *DrizzlePac/Astrodrizzle* software (Gonzaga, *et al.*, 2012), which is currently installed in the STScI on-the-fly pipeline (OTFR). This software requires accurate distortion correction in order to combine dithered WFC3 images, and thus enhance the spatial resolution and deepen the detection limit. If the geometric distortion correction, implemented in *DrizzlePac* is not sufficiently accurate, then the WFC3 image-combination process can produce blurred images and distort the under-sampled Point Spread Function (PSF).

After Servicing Mission 4 in May 2009, the astrometric calibrations of WFC3/UVIS & IR were based on two astrometric standard fields – one in the globular cluster 47 Tuc (Anderson, 2007) and the other in the Large Magellanic Cloud (Anderson, 2007). 47 Tuc and the Large Magellanic Cloud were observed with the F606W UVIS and F160W IR filters, with a variety of dithers. The derived WFC3/UVIS geometric distortion, as described in detail by Kozhurina-Platais *et al.* (2009), is presented as a fourth-order polynomial model and is accurate to a precision level of 0.1 pixel in the UVIS and IR or (4 *mas* and 10 *mas*, respectively).

In Cycle 18, a standard astrometric catalog based on ACS/WFC observations of the globular cluster ω Cen (Anderson & van der Marel, 2010) has been used to examine the multi-wavelength geometric distortion of WFC3/UVIS and IR channels. Thus, the globular cluster ω Cen was observed through 10 UVIS and 5 IR filters (CAL–11911, PI Sabbi, CAL–11928, PI Kozhurina-Platais). In Cycle 19, (CAL–12353, PI Kozhurina-Platais), ω Cen was observed with additional new UVIS filters and IR filters. In Cycle 20 (CAL–13100, PI Kozhurina-Platais), ω Cen was observed with the F606W and F621M UVIS filter. Therefore, for each of the 14 calibrated UVIS filters, unique polynomial coefficients of the geometric distortion in the form of Instrument Distortion Correction Tables (IDCTAB, Hack & Cox 2001) are available for use in ST software *DrizzlePac* and OTFR.

The IDCTAB given by the 4th order polynomial accounts for the *macro-distortion* due to the optical assembly of HST. On top of this large-scale geometric distortion, there is a *micro-distortion*, which consists of fine-scale systematics in the residuals from the best-fit polynomial solutions. These systematic residuals typically extend to ∼0.15 pixel and vary in amplitude depending on the location within a CCD chip. Such residuals cannot be removed by a polynomial model. These fine–scale and low–amplitude distortions are the result of: 1) a detector defect caused by the manufacturing process and 2) the imperfections of the filter itself. For example, in the case of WFPC2, a small manufacturing defect occurs

at every $\sim$ 34th row of each of the WFPC2 chips (Anderson & King, 1999). This defect introduced errors in photometry at the level of 0.01-0.02 magnitude, and periodic errors in astrometry at about $\sim$0.03 pixel. In the case of the ACS/WFC, a similar detector defect was identified in every $\sim$68th column for each of the WFC CCD chips, which induces a periodic error in astrometry of $\sim$0.1-0.8% (Anderson, 2002). For both WFPC2 and ACS/WFC, the detector defect is a 1–D correction, in either the X or Y direction. The correction for these defects has been implemented in *Multidrizzle* and later in *DrizlePac/Astrodrizzle* as a 1–D linear interpolation, which is applied prior to the large-scale distortion (polynomial model) correction. The WFC3/UVIS detector defect due to lithographic-mask pattern is imprinted onto the detector itself. The lithographic-mask pattern is a 2–D defect and, therefore, requires a bi-linear interpolation in *DrizzlePac/Astrodrizzle*. Because of that, *Astrodrizzle* has required modification to account for the 2–D nature of this defect.

Here, we present the analysis and results of the lithographic-mask pattern correction in the WFC3/UVIS X,Y raw positions, and its implementation in *DrizzlePac/Astrodrizzle* software. The lithographic-mask pattern with fine-scale structure has been modeled using a look-up table, which then can be bi-linearly interpolated at any point in WFC3/UVIS images by *DrizzlePac/Astrodrizzle*.

2. WFC3/UVIS Micro-Distortion

2.1. Observations and Reductions

The standard astrometric catalog in the core of globular cluster ω Cen was used to perform a multi-wavelength geometric distortion calibration of UVIS and explore its time dependency. The tangent–plane projection type (rectangular coordinate system) positions of stars in the standard astrometric catalog are globally accurate to $\sim$0.02 ACS/WFC pixel or $1mas$ (Anderson & van der Marel, 2010). The globular cluster ω Cen was observed with the UVIS detectors near the center of the standard astrometric catalog with a large dither pattern and at different HST roll-angles (CAL-11911, PI Sabbi; CAL-12904, PI Petro; CAL-12353, PI Kozhurina-Platais; CAL-12714, PI Kozhurina-Platais; CAL-13100, P Kozhurina-Platais). The observations of ω Cen through F606W UVIS filters have a total of 60 UVIS images.

The reduction and analysis is similar to the reductions and analysis used in the SMOV UVIS geometric distortion calibration and similar to the multi–wavelength geometric distortion calibration for the UVIS filter. A detailed description of the reduction and analysis is given by Kozhurina-Platais *et al.*, (2009, 2012). Nearly 40,000 stars in each UVIS CCD chip image were used to derive the 4th-order polynomial solutions, providing an extremely well-constrained large-scale distorion solution.

2.2. WFC3/UVIS Detector Defect

After applying the best–fitting polynomial, the residuals of X and Y positions from the WFC3/UVIS observations of ωCen frame and the astrometric standard catalog are essentially flat, i.e. all large–scale residuals are successfully removed. Nevertheless, there are noticeable fine–scale systematic residuals from these best–fit polynomial solutions. In order to visualize these residuals, we examined the X and Y residuals from one of the F606W images in vertical and horizontal slices through UVIS1 and UVIS2 in steps of δX=512 pixels in X and δY = 256 pixels in Y and a width of 128 and 64 pixels, respectively.

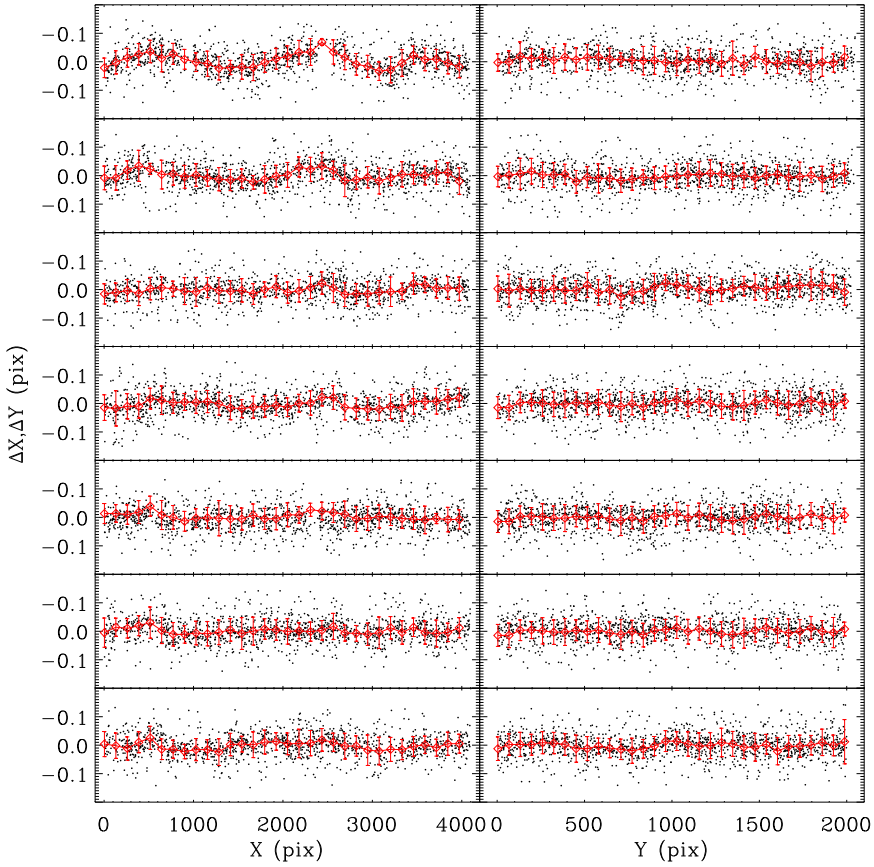

Fig. 1.— Narrow slices of X and Y residuals centered at the selected X positions with the step of 512 pixels in X and at the selected δY with the step of 256 pixels in Y (from the top to the bottom 1792, 1536, 1280,1024, 768, 512, 256) through the UVIS2 chip. The residuals are from the best–fit polynomial solution for an F606W image. The X,Y coordinates are given in WFC3/UVIS pixels.

As seen in Figures 1 and 2, the X and Y residuals for UVIS1 and UVIS2 CCD chips show a complicated structure, depending on the location within the CCD, with a typical

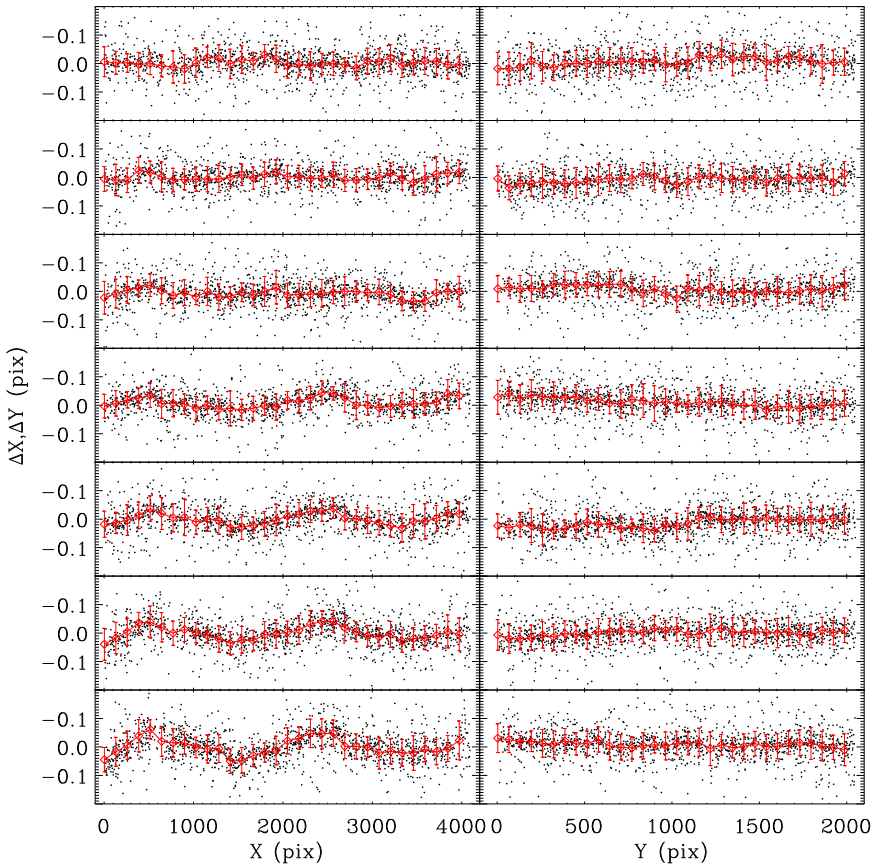

Fig. 2.— The same as in Fig. 1, but for UVIS1.

amplitude of ∼0.15 pixel and coherence scale of ∼ 500 pixels, which would require a very high order polynomial to remove it.

In order to investigate the nature of such a complicated structure, we looked at X & Y residuals in each of the 14 UVIS filters. For all 14 calibrated filters, a noticeable patchy fine-scale systematic trend with the average coherence scale of ∼700×1000 pixels is seen in the residuals from the best-fit polynomial solutions. Figure 3 shows the post-solution X and Y residuals as vector diagrams for 4 selected UVIS filters. The apparent pattern persists from filter to filter, which is an indication that this feature is related to the detector itself. On top of this geometric pattern, there is also a noticeable fine-scale systematic trend varying from filter to filter. This variation has a coherence scale of ∼100 pixels with a typical amplitude of 0.05 pixel. However, as seen in Figure 3, the F606W filter has less structure in the residual map than the F775W, for example. Smaller and less complicated structure in the F606W residuals map is an indication of small irregularities due to manufacturing of the filter itself. Because of such small irregularities in the filter, the F606W filter has been chosen as the base for the UVIS distortion solution and the other filters are essentially tied to F606W.

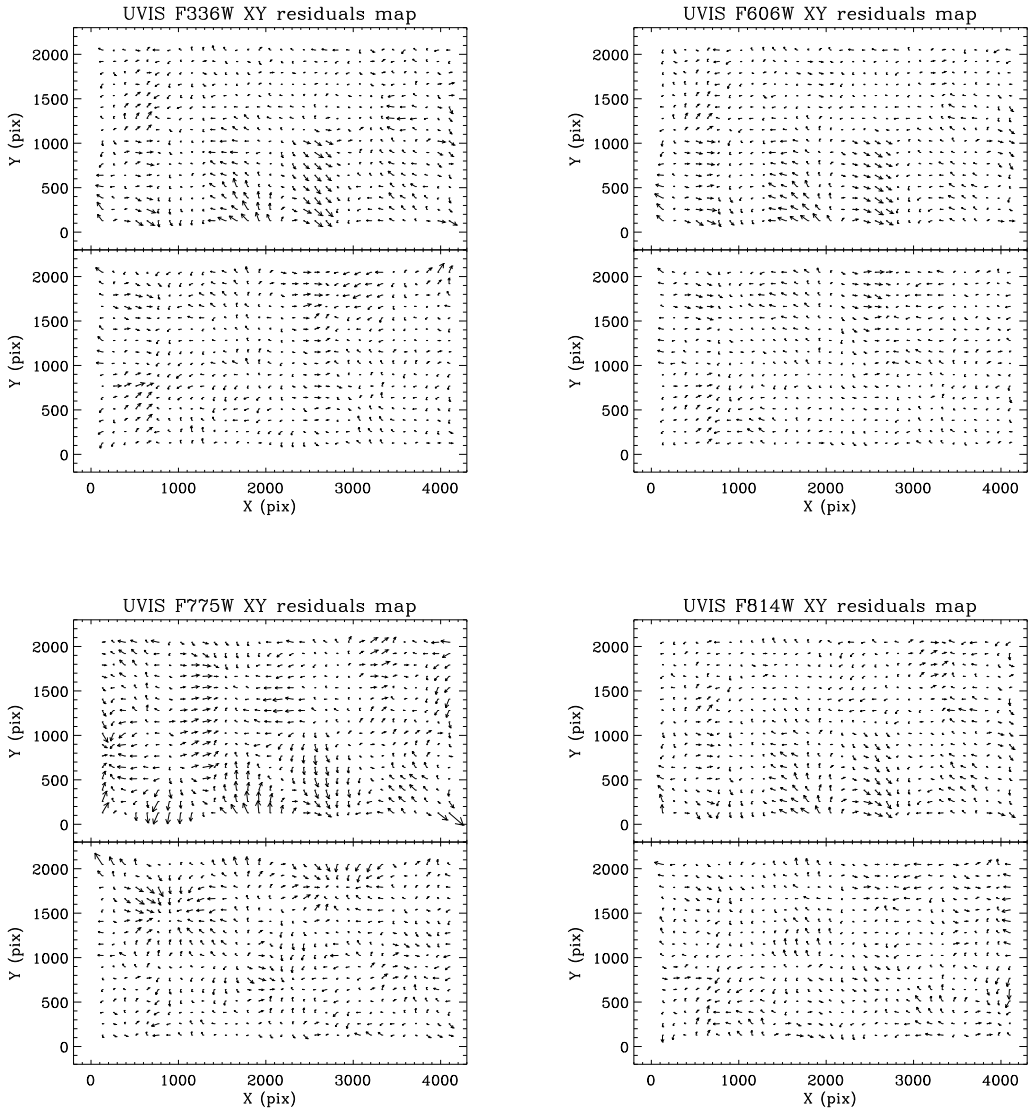

Fig. 3.— 2D X and Y residual map between the UVIS positions and the standard astrometric catalog after the geometric distortion is removed. The top panel shows the X and Y residuals for the WFC3/UVIS1 CCD chip and the bottom panel X, Y residuals for WFC3/UVIS2 CCD chip. From top to the bottom, and from left to right, the residuals maps are for UVIS F336W, F606W, F775W and F814W filters. The largest vector is ∼0.35 pixel, magnified by a factor of 2000. The units are WFC3/UVIS pixels.

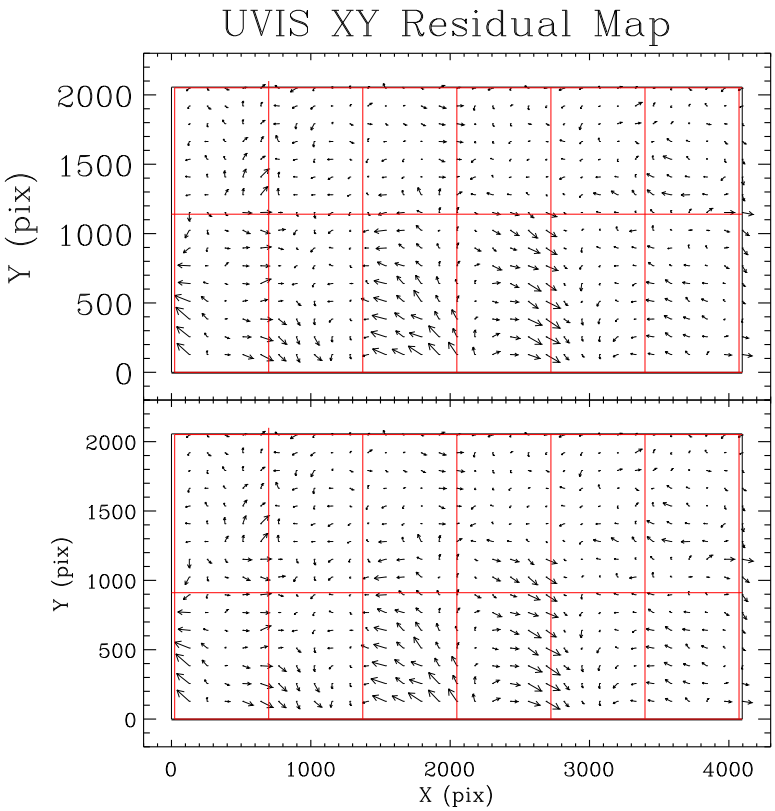

Fig. 4.— 2D XY residual map between F606W UVIS filter positions (corrected for geometric distortion) and the standard astrometric catalog. The top panel shows the X and Y residuals for the WFC3/UVIS1 CCD chip and the bottom panel X and Y residuals for WFC3/UVIS2 CCD chip. The approximate boundaries of lithographic-mask pattern with the size of ∼700×1000 pixels are over-plotted by red boxes. The largest vector is ∼0.15 pixel, magnified by a factor of 2000. The units are WFC3/UVIS pixels.

Figure 4 shows a complicated structure placed in a fixed-size box, representing the estimated size of lithographic-mask pattern on the flat-field images. The lithographic-mask pattern has period of 675 pixels in the X direction and 911 & 1140 pixels in the Y direction, which are placed symmetrically with respect to the gap between the two UVIS CCD chips. The boundaries of a mask used for photo-lithography are clearly evident. The discontinuities between the vectors coincide with the lithographic-mask boundaries (red lines) as measured in the flat-field image. The photo-lithographic mask pattern on the UVIS detector is actually a detector defect imprinted into detector itself during the process of a photo-lithographic-mask projection on CCD. This defect appears to be similar to that of the WFPC2 CCD and ACS/WFC CCD chips (Anderson & King, 1999, Anderson, 2002).

2.3. Fine-Scale Solution and Look-Up Table

The complicated structure in residuals after applying the best-fit polynomial discussed in the previous section cannot be modelled by a high order polynomial. A simple way to remove any fine-scale variations is to construct a look-up table, which then can be linearly interpolated at any point in the WFC3/UVIS image. The WFC3/UVIS lithographic pattern and its correction is decribed by Bellini *et al.*, (2011), who provide a combined look-up table for both detector defect and the fine-scale filter structure. However, the detector defect is filter independent and because of that it should always be applied to raw X & Y UVIS positions first, before consideration a filter-dependent correction. Thus, we constructed a separate look-up table to deal only for detector-defect correction.

The computed residuals of X and Y positions from the best polynomial solutions in the F606W filter, as described in Sect.2.2, were used to construct the initial look-up table for the detector defect. There are a couple of restrictions on the structure of such a look-up table:

- it should accommodate the format limitations imposed by *DrizzlePac/AstroDrizzle* and the STScI of-the-fly pipeline;
- it should optimize extraction of the 2-D detector defect structure over both WFC3/UVIS CCD chips;

Owing to the limited number of available residuals, they should be binned such that the lithography-mask pattern is adequately represented. We ran a few tests to find the optimal array size for a look-up table. The first test, using an array of 64×32 points with a bin size of 64×64 pixels, showed that the lithography signal in the residuals decreases due to the increased noise level. Another test, using a large bin of 256×256 pixels and an array of 16×8 points, resulted in smoothing out the lithographic-mask pattern. The best sampling is provided by using 128×128-pixel bins over an array of 32×16 points. This provides an optimal sampling of the lithographic pattern and has enough stars at each grid point to construct the look-up table. For any given grid point, there were ∼200-300 stars to calculate an accurate vector of residuals in the form of sigma-clipped average of all residuals within a radius of 64 pixels. The look-up table and its interpolation scheme for a use in *DrizzlePac/Astrodrizzle/TweakReg* has to be comply with the constrains of software and the STScI on-the-fly pipeline (OTFR). Because of that, the chosen bin size of 128×128 pixels is not able to match exactly the boundary between the adjacent lithographic-mask patterns.

The final look-up table was constructed using the residuals after removal of the lithographic-mask pattern from the raw X and Y positions and obtaining the improved polynomial coefficients of geometric distortion.

Figure 5 shows the residual map in F606W filter after the lithographic-mask pattern correction was applied. As can be seen in the residual map, there is no longer any indication

of the lithographic-mask pattern, with the exception of some small correlated offsets at the boundary of patterns. The residual map looks smooth, the noise is reduced, and the spatial structure is essentially absent.

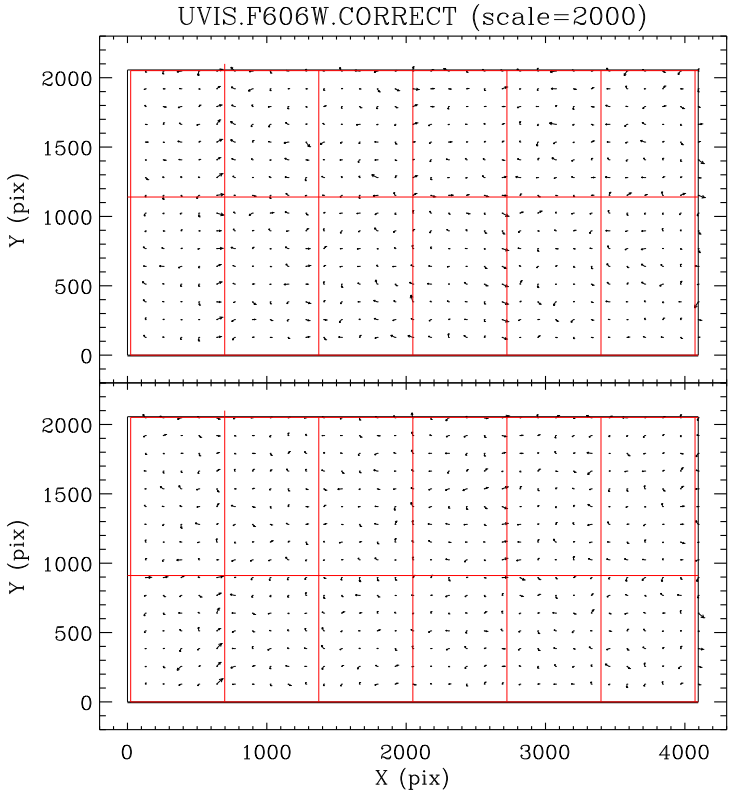

Fig. 5.— The same as in Figure 4, but after the correction for lithographic-mask pattern The largest vector is ∼0.05 pixel, magnified by a factor of 2000. The units are WFC3/UVIS pixels.

Thus, the derived look-up table is a two-dimensional correction over an array of 32×16 points, throughout the 4096×2051 pixel image, which can be linearly interpolated at any point in the WFC3/UVIS image. The resulting look-up table derived from observations taken through the F606W filter was used to correct the raw X and Y positions for detector defects in each of the other 14 calibrated UVIS filters. Since this new correction is applied to all 14 calibrated filters, the new filter-specific geometric distortion solutions for each of these filters were generated, yielding a new improved polynomial coefficients of the UVIS geometric distorion in the form of IDCTAB.

3. Detector Defect Correction Implementation in *DrizzlePac* Software

As described by Hack *et al.* (2012), calibration of the distortion for HST observations is recorded and applied through the reference files, listed in the primary header of `*_flt.fits`. The following reference files for distortion are available in the header: *i*) D2IMFILE which is the detector defect reference file; *ii*) IDCTAB is containing polynomial coefficients of the geometric distortion; *iii*) NPOLFILE is giving additional filter–dependent distortion. All of these corrections are part of the World Coordinate System (WFC) transformation in the new software routines *DrizzlePack* (Gonzaga, *et al*, 2012). D2IMFILE is represented by a 1–D array which is applied to each row/column on WFPC2 and/or ACS/WFC, respectively. The convention adopted for WFPC2 and ACS/WFC cannot describe more complex 2–D detector defect correction which would be required for the WFC3/UVIS. Because of that, the original implementation, described in *http* : *//stsdas.stsci.edu/tsr/stwcs/fits_conventions/d2imcorr*, was extended to support the 2–D corrections represented by a 2–D look-up table, separately for each CCD chip. This 2–D look-up table is bi-linearly interpolated and implemented in PyWCS and STWCS (Python/PyRaf tasks) and converted into the FITS format as a reference file. The keyword of this correction is D2IMFILE in the primary header.

Thus, the reference file D2IMFILE as a detector defect correction, is used for pixel-by-pixel correction prior to the polynomial coefficients distortion, and by bi-linear interpolation in *DrizzlePac/Astrodrizzle/TweakReg* software.

4. Test with *DizzlePac* Software

The new software *DrizzlePac* (Gonzaga, *et al.*, 2012) developed recently by STSDAS has replaced the old *MultiDrizzle* software. The *DrizzlePac* software is designed to align and combine the HST images. In *DrizzlePac* there are a few tasks that can be used to perform astrometric solution between the HST images and to make the transformations of HST images such as a shift, rotation and scale in order to find preliminary astrometric input for *Astrodrizzle* to align and combine HST images. One of such tasks, is *TweakReg*, an automated interface to compute the residuals, shift and rotation between HST images. This task uses, `*_flt.fits` files as input, finds X and Y positions in these images (similar to IRAF/DAOFIND), corrects X and Y positions for geometric distortion using the reference files (D2IMFILE & IDCTAB) from the header, and solves for a shift, scale and rotation between the input images (similar to IRAF task XYXYMATCH). The new derived reference files, D2IMFILE (detector defect correction) and IDCTAB with new polynomial coefficients, corrected for the lithographic- mask pattern, were then tested here with *DrizzlePac/TweakReg*.

To test these newly derived refernce files (D2IMFILE and IDCTAB), we took pair of of ω Cen observations with large POSTARGs of +/-40″. Such a large shift between two UVIS images have the advantage of overlapping UVIS1 *vs.* UVIS1, UVIS1 *vs.* UVIS2 and UVIS2

vs. UVIS2. Such overlapped areas between two UVIS images with large shift, will be served to validate correction for the lithographic-mask pattern.

Figures 6–8 show the residuals of X and Y positions in the overlapping area between two UVIS images, before and after correction for the lithographic-mask pattern.

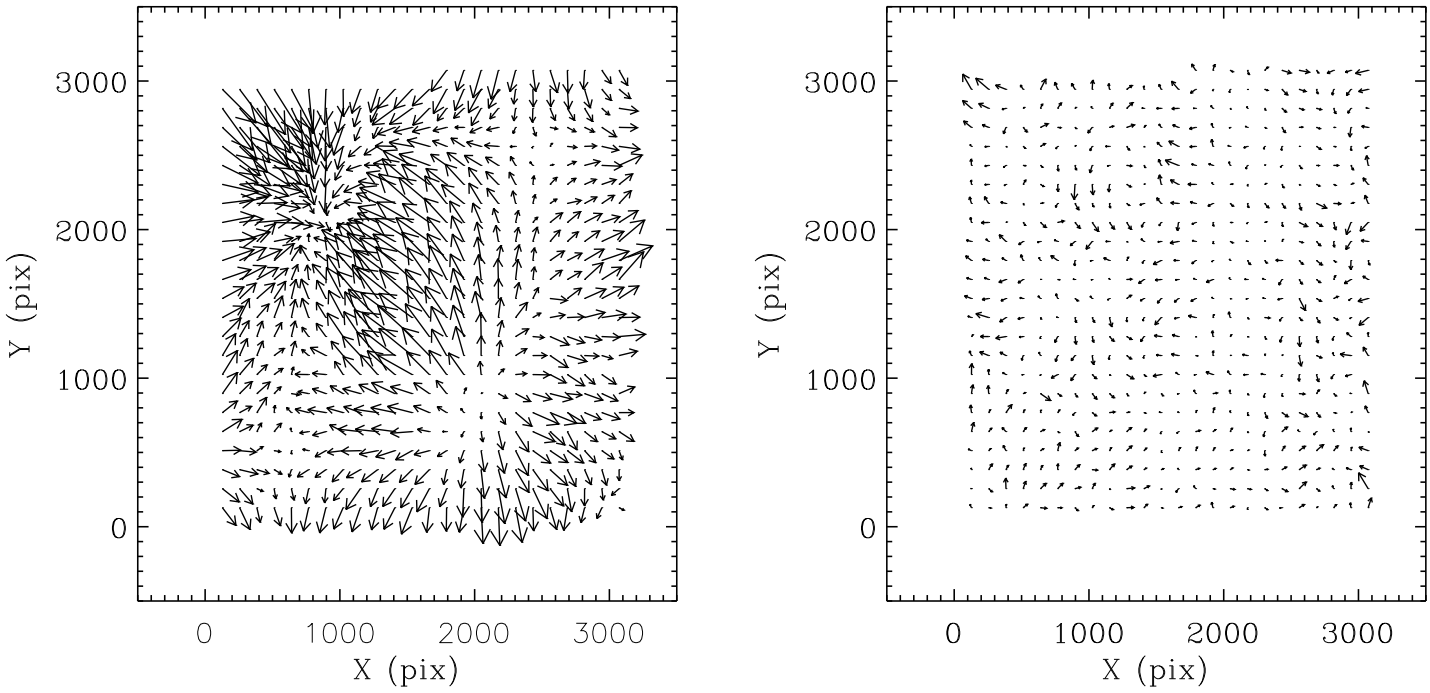

Fig. 6.— 2-D X and Y residual map between two drizzled F336W images with large POSTARG. On the left, the residuals before the detector defect correction. On the right, the residuals after the detector defect correction. The largest vector in the left panel is ∼0.25 pixel and the largest vector in the right panel is ∼0.07 pixel, both magnified by a factor of 2000. The units are WFC3/UVIS pixels.

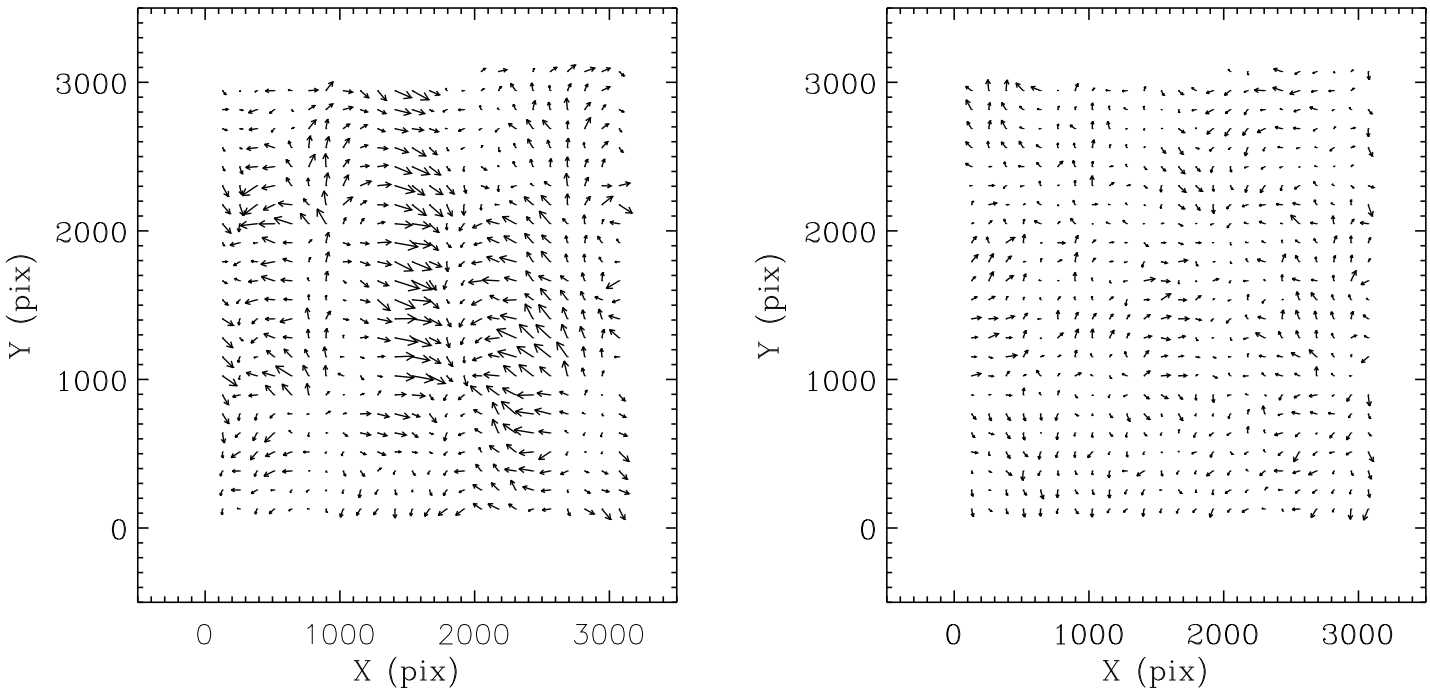

Fig. 7.— The same as in Fig.6 only for two F606W drizzled images. The largest vector in the left panel is ∼0.15 pixel and the largest vector in the right panel is ∼0.05 pixel, both magnified by a factor of 2000. The units are WFC3/UVIS pixels.

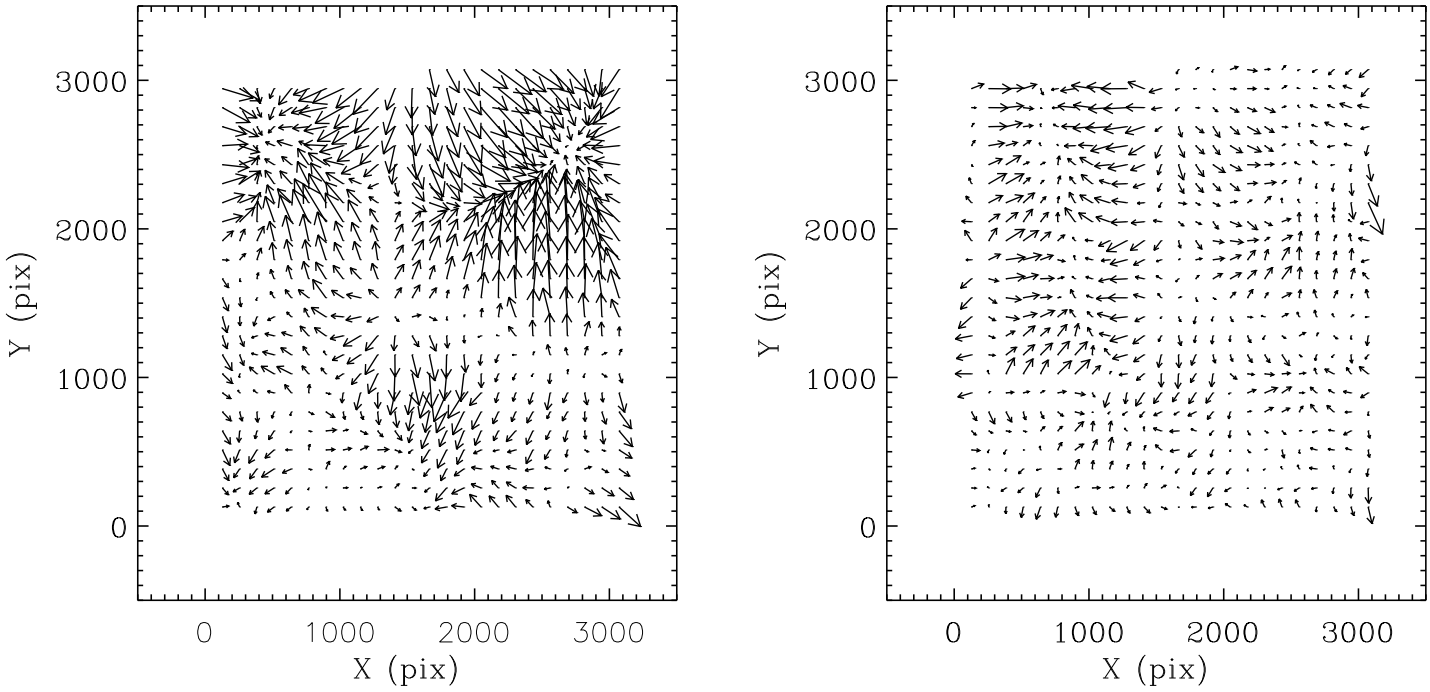

Fig. 8.— The same as in Fig.6 only for two F775W drizzled images. The largest vector in the left panel is ∼0.35 pixel and the largest vector in the right panel is ∼0.08 pixel, both magnified by a factor of 2000. The units are WFC3/UVIS pixel.

As can seen in Figures 6 - 8 (left pannels), the residuals without the detector defect correction have a large–scale structure with an amplitude from of ∼0.15 to ∼0.35 pixel depending on the positions in UVIS CCD chips. This large–scale structure also depends on the filter. After the detector–defect correction (Figs. 6 – 8, right pannels), the large-scale structure is reduced to ∼0.07 pixel and less. Thus, the residuals of X and Y positions in the overlapping areas between two UVIS images before and after correction shows significant improvement.

However, as seen in Figure 6–8, some fine-scale remains structure due to filter irregularities. These systematic residuals are typically ∼0.05 pixel in amplitude and vary with a spatial frequency of ∼100 pixels. In the case of F775W filters, the residuals are more irregular, and the amplitude in some places can reach about ∼0.1 pixel.

Thus, applying the UVIS lithographic-mask pattern correction, there is achievement in the improvement by about 30-60% in precision of the UVIS distortion correction. The *RMS* of positions residuals is now less than 0.05 pixel in each coordinate for well measured stars in UVIS drizzled images.

5. Conclusion

More than 4 years of observations of ω Cen with F606W UVIS filter have been used to examine the WFC3/UVIS detector defect, related to the lithographic-mask manufacturing process. These observations have been used to consruct a look-up table-based corection and thus remove a fine-scale systematics in X and Y positions due to this detector defect. After applying this correction to each of the 14 calibrated UVIS filters, new polynomial coefficients were obtained, which now more accurately represent the WFC3/UVIS geometric distortion.

After applying the detector–defect correction (D2IMFILE) and the newly derived IDCTAB, there is a significant 30-60% improvement in the distortion correction. This new solution can be used in *STSDAS/DrizzlePac* for: 1) accurate stacking of various WFC3/UVIS images taken with a different dither pattern and orientation; 2) rejection of CRs with higher accuracy and precision in the final drizzled UVIS images; 3) enhancement of the spatial resolution; 4) deepening of the detection limit. The geometric distortion can be successfully corrected at the level of 0.05 pixel equal to $2mas$ in UVIS images.

The next step in improvement of UVIS geometric distortion would be implementation of a look-up table (NPOLFILE reference file for filter–dependent distortion) to remove the fine–scale variations due to the irregularities in UVIS filters. The F775W filter in particular could benift for such improvement.

Ultimately, the precision level in WFC3/UVIS distortion correction mainly depends on the accuracy with which X and Y positions can be measured on re-sampled WFC3/UVIS images.

Acknowledgments

We express our gratitude to Jay Anderson for reviewing this ISR and for his useful comments and suggestions which improved significantly the clarity of ISR. We greatly appreciate many discussion with John MacKenty about the WFC3/UVIS lithographic-mask and its properties. We gratefully acknowledge Jennifer Mack and Mike Dulude for the regression test with newly derived reference files and DrizzlePac/TweakReg software.

References

Anderson, J., King, I., 1999, PASP, 111, 1095-1098

Anderson, J., 2002,in "2002 HST Calibration Workshop", eds S.Arribas, A. Koekemoer, B. Whitmore, (Baltimore:STScI)

Anderson, J., 2007, ACS Instrument Science Report, ACS-ISR-07-08 (Baltimore:STScI)

Anderson, J, 2007, (private communication)

Anderson, J., & van der Marel, R.P., 2010, ApJ, 710, 1032-1062

Bellini, A., Anderson, J., Bedin, L., 2011, PASP, 123, 622-637

Gonzaga, S., Hack, W., Fruchter, A., et.al., 2012, "The DrizzlePac Handbook". (Baltimore: STScI)

Hack, W., & Cox, C., 2001, ACS-ISR-01-08 (Baltimore:STScI)

Hack, W., Dencheva, N., Fruchter, A., Greenfield, P., 2012, Technical Sowtware Report, TSR 2012-01, (Baltimore:STScI)

Fruchter, A., Hook, P., 2002, PASP, 114, 144-152

Fruchter A., Sosey, M., et.al., 2009, " The MultiDrizzle Handbook", v.3, (Baltimore:STScI)

Koekemoer, A.,M., Fruchter, A., Hook, R.,N., Hack, W., 2002, in "2002 HST Calibration Workshop", eds A.Arribas, A. Koekemoer, B.C, Whitmore (Baltimore:STScI), p.337

Kozhurina-Platais, V., Cox, C., McLean, B., Petro, L., Dressel, L., Bushouse, H., Sabbi, E., 2009, WFC3 Instrument Science Report, WFC3-ISR-09-33 (Baltimore:STScI)

Kozhurina-Platais, V., Cox, C., Petro, L., Dulude, M., Mack, J., 2010, in "2010 HST Calibration Workshop", eds S. Deustua, C. Oliveira (Baltimore:STScI)

Kozhurina-Platais, V., Dulude, M., Dahlen, T., Cox, C., Sabby, 2012, WFC3 Instrument Science Report, WFC3-ISR-2012-07 (Baltimore:STScI)